Proceedings on Automation in Medical Engineering
Proc AUTOMED, 2026, Vol. 3, No 1, Article ID 2475, 2 Pages

Infinite Science Publishing

Multi-scale particle image velocimetry for respiratory flows and comparison with numerical simulations

S. B. Oskouei[1,2*], V. Viola[1], C. Jordan[2], T. Baumgartner[1], A. Aloy[3], R. Kölbl[4], M. Harasek[2] and M. Gföhler[1]

[1] *Institute of Engineering Design and Product Development, TU Wien, Vienna, Austria*
[2] *Institute of Chemical, Environmental and Bioscience Engineering, TU Wien, Vienna, Austria*
[3] *Institute of Fluid Mechanics and Heat Transfer, TU Wien, Vienna, Austria*
[4] *Carl Reiner GmbH, Vienna, Austria*

[*] *Corresponding author, email: seyedmohsen.oskouei@tuwien.ac.at*

Abstract: This work presents a multi-scale experimental validation framework using macro- and micro-scale Particle Image Velocimetry (PIV). Rigid bifurcation models are fabricated using high-resolution DLP 3D printing. Flow fields are analyzed under steady and unsteady conditions, including high-frequency flow (Wo = 4.3) and low-Reynolds microflows. Comparisons of velocity profiles demonstrated agreement between experimental measurements and Computational Fluid Dynamics (CFD) results.

I. Introduction

Due to their time-dependent nature, complex geometries, and turbulence, respiratory flows present a significant challenge in CFD. This challenge becomes more prominent in high-frequency flow fields, such as those found in high-frequency jet ventilation. Furthermore, due to the fractal branching of the respiratory bronchi, the flow field experiences a multi-scale geometrical resizing. Consequently, flow regimes transition from higher Reynolds numbers in the upper generations to significantly lower numbers in the lower generations [1]. In this work, macro- and micro-scale PIV measurements are used to provide experimental measurements at different Reynolds numbers (Re).

II. Materials and methods

II.I. Test piece preparation

DLP 3D printing (using an Asiga Max 27) is utilized to create macro- and micro-scale test pieces. The macro-scale test piece is a branch with an inner diameter of the parent branch being 8 mm and the child branches with an inner diameter of 6 mm. The child's branches are positioned on the same plane with a 70° angle between them. To enable easy post-processing (sanding), the test piece is printed inside a prism with flat surfaces. For the micro-scale test piece, the same printer is used to print four branches with a width of 0.4 mm and depth of 3 mm. Figure 1a and b show the post-processed 3D-printed macro- and micro-scale models, respectively.

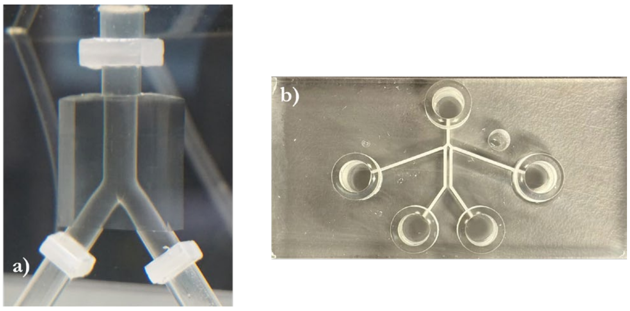

Figure 1: Macro-scale (a) and micro-scale (b) test pieces

II.II. PIV setups

As illustrated in Figure 2, the experimental setup employs a computer-controlled syringe pump to generate custom time-dependent flow profiles. The working fluid is seeded with $9-13\ \mu m$ hollow glass spheres ($\rho\ =\ 1100\ kg/m^3$, LaVision GmbH). Illumination is provided by a Litron Bernoulli B-PIV laser, which emits a beam passed through cylindrical and spherical lenses to create a thin light sheet focused on the test section midplane. A TSI LaserPulse Synchronizer coordinates the laser pulses with an Andor Zyla 5.5 sCMOS camera, positioned perpendicular to the light sheet, to capture particle images at 15 Hz. The resulting data is subsequently post-processed using TSI Insight 4G software.

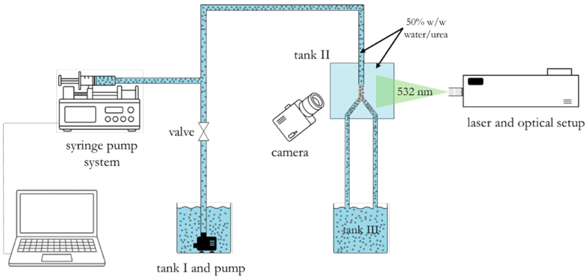

Figure 2: Macro-scale PIV setup

Figure 3 illustrates the micro-scale experimental setup, where the flow is seeded with ThermoFisher Fluoro-Max red 3 μm polystyrene fluorescent particles. In contrast to the macro-scale configuration, illumination is delivered via a fiber optic cable positioned on the same side as the imaging optics (epifluorescence mode). An Olympus IX73 inverted microscope equipped with a 4 × magnification objective is employed to capture the flow field at the microchannel midplane.

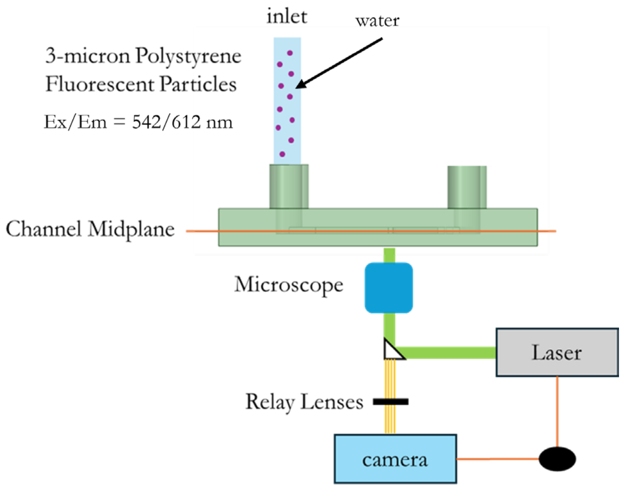

Figure 3: Micro-scale PIV setup

III. Results and discussion

Figure 4 compares the steady profiles at the parent and children branching between macro-scale PIV and CFD for three different Re.

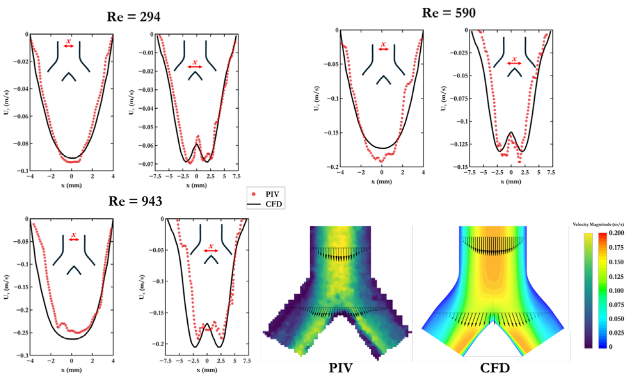

Figure 4: Comparison between steady macro-scale PIV and CFD velocity profiles at different Reynolds numbers and velocity contour at Re = 943

Figure 5 compares the unsteady velocity profiles at Re = 140 and Womersley (Wo) of 4.3, which represents a high-frequency ventilation case. At these Wo, a time shift between the velocity and pressure fields takes place.

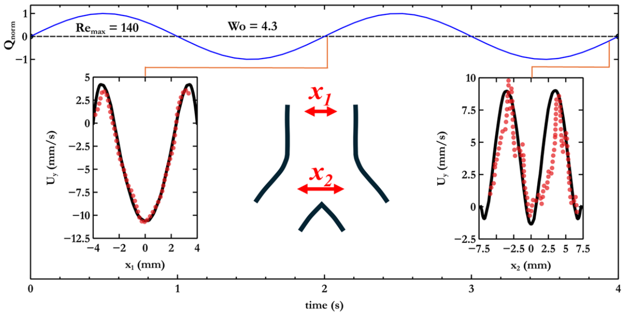

Figure 5: Comparison between unsteady macro-scale PIV and CFD results at Re = 140 and Wo = 4.3

Figure 6 compares the velocity magnitude contours between PIV and CFD for the micro-scale measurements at Re = 20.

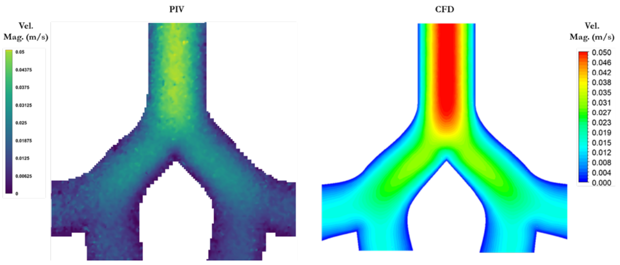

Figure 6: Velocity magnitude contour comparison between the micro-scale PIV and CFD at Re = 20

The provided comparison presents viable validation tools at different respiratory scales for steady and unsteady flows.

IV. Conclusions

Macro -and micro-scale PIV was used to measure the flow field at steady and unsteady conditions for bifurcations in respiratory flows. Velocity profile and contour comparisons with CFD simulations revealed good agreement between the numerical results and experiments. Future studies will focus on capturing unsteady turbulent flow at macroscopic scales and unsteady laminar profiles at microscopic scales.

Author's statement

Research funding: The authors state that this research was partially funded by the Austrian Research Promotion Agency (FFG). Project: HiELuVent, grant number FO999903605. Conflict of interest: The Authors state no conflict of interest. Informed consent: Informed consent has been obtained from all individuals included in this study. Ethical approval: No human or animal participation in this study.

References

[1] Z. Chen, S. Parameswaran, Y. Hu, Z. He, R. Raj, and S. Parameswaran, "Numerical Simulations of High-Frequency Respiratory Flows in 2D and 3D Lung Bifurcation Models," *International Journal for Computational Methods in Engineering Science and Mechanics*, vol. 15, no. 4, pp. 337–344, July 2014, doi: 10.1080/15502287.2014.904454.